Accounts

Cyclic π-Conjugated Systems Annelated with Bicyclo[2.2.2]octene: Synthesis, Structures, and Properties

Koichi Komatsu

Institute for Chemical Research, Kyoto University, Uji, Kyoto-fu 611-0011

(Received August 31, 2000)

This article presents an account of studies on the synthesis and properties of the cyclic π-conjugated systems annelated with bicyclic σ-frameworks. Particular emphasis is placed on π-systems carrying a positive charge, which are remarkably stabilized by complete annelation with bicyclo[2.2.2]octene. In such systems, not only the kinetic effects but also electronic effects due to σ–π conjugation strongly affect the properties of the π-systems. The thermodynamic properties, redox behavior, and the X-ray crystal structures are discussed. The cyclic π-systems studied include hydrocarbon molecules such as benzene and a series of benzenoid condensed aromatics, seven-membered ring non-benzenoid aromatic cation, i.e. tropylium ion, cyclooctatetraene, a spiro-connected cyclopentadiene, and dehydroannulenes. The study is further extended to systems containing heteroatoms such as 1,4-dithiin, metallacycloheptatrienes, and silatropylium ion.

The π-electron plays a dominant role in the chemistry of cyclic π-conjugated systems, whereas the σ-frameworks serve to control the shape of the π-systems. However, the σ-frameworks can also work in a different way. When a C–C σ-bond is located in a position parallel to the *p*-orbital, the C–C hyperconjugation becomes effective, particularly interacting with the *p*-orbital that is empty. Such effects have, for example, been demonstrated theoretically for the 1,1-dimethylpropyl cation[1] and experimentally for the 1-adamantyl cation.[2]

Thus, it is of particular interest to investigate the properties of the cyclic π-conjugated systems surrounded by rigid σ-frameworks, such as bicycloalkenes. In such systems not only the inductive effects but the σ–π conjugative effects (i.e., the C–C hyperconjugative effects) can operate, because the bicycloalkenes can provide σ-bonds which are rigidly fixed at the position nearly parallel to the *p*-orbitals of the π-system.

In this account, a review is made with regard to the cyclic π-systems annelated with bicyclo[2.2.2]octene, with particular attention placed on the stabilization of the positively charged systems.

1. Annelation with Bicyclo[2.2.2]octene

Annelation with multiple units of bicycloalkene not only brings about the electronic effects mentioned above, but it can sterically, i.e. kinetically, protect the central π-system. Such units can also exert the so-called "Bredt's-rule protection"[3] against decomposition of the positively charged π-system: decomposition via deprotonation from the α-position of the substituents is inhibited because such an event would result in the formation of a bridgehead olefin and violation of Bredt's rule.

What would be the most appropriate size of the bicycloalkene to be attached to the π-system? The effect of the annelating bicycloalkene was examined by comparing the thermodynamic stability, expressed by the pK_{R^+} value, and the reduction potential of a series of substituted tropylium ions as a representative cationic π-conjugated cyclic system.[4,5] The *t*-butyl group can be taken as a typical inductively electron-donating group, while the cyclopropyl group is considered as a typical σ-conjugative group. As shown by the pK_{R^+} values given in Table 1, the cyclopropyl group can stabilize the tropylium ion much more strongly than the *t*-butyl group.[4] The bicyclo[2.1.1]hexene (abbreviated as BCH) unit is highly strained, with its σ-bonds having considerable *p*-character. Thus, its annelation was antici-

Table 1. Values of pK_{R^+} and Reduction Potential for the Tropylium Ions **1–5**

Cation	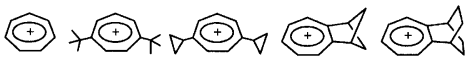				
	1	**2**	**3**	**4**	**5**
pK_{R^+} [a]	3.88	5.42	7.63	5.10	7.80
E_{red} [b]	−0.51	−0.72	−0.76	−0.71	−0.765
Ref.	4	4	4	5	5

a) Measured in 50% aq MeCN. b) Cathodic peak potential (V vs. Ag/Ag^+) measured in MeCN containing Bu_4NClO_4 (0.1 M); scan rate, 0.1 V s^{-1}.

pated to be as effective as two cyclopropyl groups in stabilizing the cation. However, the pK_{R+} value of the BCH-annelated tropylium ion **4** was much lower than that of dicyclopropyltropylium ion **3**: this is ascribed to the internal angle strain of the tropylium ring imposed by the BCH annelation. Instead, annelation with bicyclo[2.2.2]octene (abbreviated as BCO), which is not so strained and can provide σ-bonds that are nearly parallel to the *p*-orbital of the π-system, was found to stabilize the tropylium ion as effectively as two cyclopropyl groups.[5] From these data, annelation with multiple units of bicyclo[2.2.2]octene (BCO) was expected to be highly effective for stabilization of cyclic π-conjugated systems having a positive charge.

2. Benzenes Tris-Annelated with Bicycloalkenes

The benzene derivatives that are fully annelated with bicycloalkenes such as **6**,[6] **7**,[7] **8**,[8] **9**,[9] **10**,[10] and **11**[11] have so far been synthesized (Chart 1). These benzenes were formally produced by cyclotrimerization of each of the bicycloalkene units. Benzene **7** was assumed to be formed by the direct trimerization of highly strained bicyclo[2.2.1]heptyne.[7] For the formation of benzenes **9** and **10**, the intermediate formation of bicyclo[2.2.2]octyne and its benzo-derivative was experimentally confirmed by trapping with diphenylisobenzofuran.[9b,10] The bicyclooctyne, however, does not cyclotrimerize by itself but undergoes stepwise oligomerization, as shown in Scheme 1: the alkyne inserts into the C–Li bond of each precursor and the in-situ lithium/bromine exchange furnishes a series of BCO oligomers **12** (n = 2–5).[9b] Benzene **9** was synthesized by the reductive cyclization of the dibromide of BCO trimer (Scheme 2).[9] Recently a high-yield synthesis of benzene **9** and "mixed" tris-annelated benzenes was reported, which utilizes the Grignard coupling and electrocyclization.[12]

Among these benzene derivatives, the X-ray crystal structure has been determined for **6**,[6] **9**,[9a] and **11**.[11] The most characteristic feature is the remarkable bond alternation induced by the molecular strain, particularly for **6**[6] and **11**.[11] Compound **6** is important in that it is the first "bona fide" mononuclear benzenoid hydrocarbon with a cyclohexatriene-like geometry. Its chemical properties, however, have not yet been studied in depth.

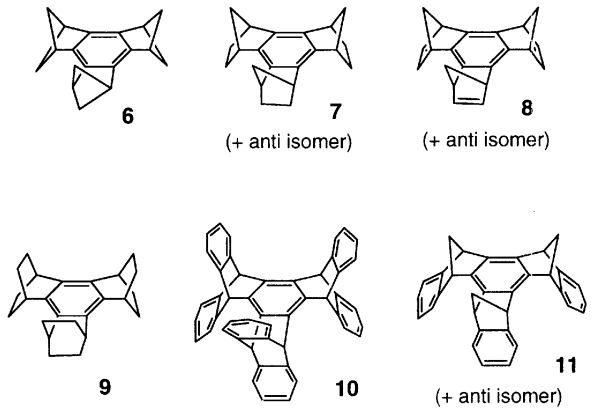

Chart 1.

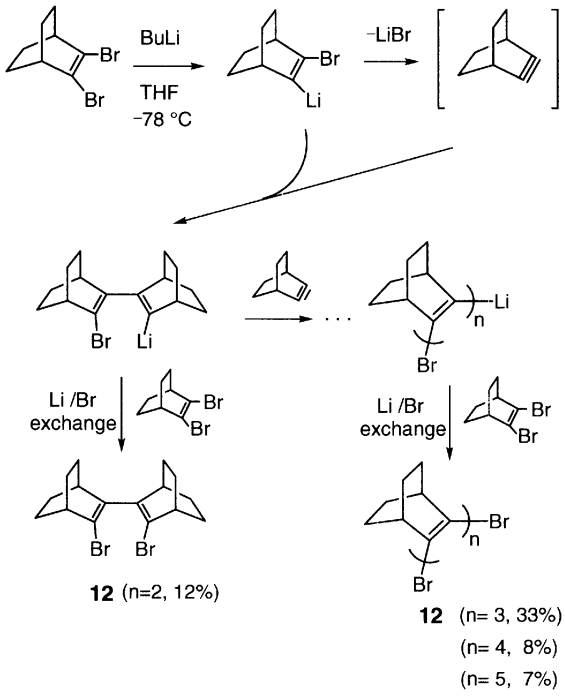

Scheme 1.

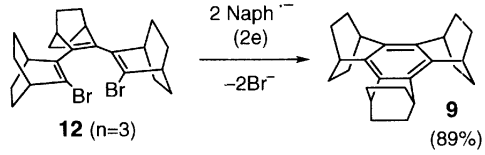

Scheme 2.

On the other hand, benzene **9** was characterized by its reversible one-electron oxidation as observed by cyclic voltammetry; $E_{1/2}$ + 1.25 V vs. Ag/Ag$^+$ in acetonitrile[9b] (+1.08 V vs. Fc/Fc$^+$ in 1,1,2,2-tetrachloroethane).[13] The electrolytically produced radical cation exhibited a 13-line ESR signal due to the coupling with twelve *anti*-protons of the ethano bridges.[9b]

The chemical one-electron oxidation of **9** with $SbCl_5$ allowed the isolation of **9**$^{\bullet+}$ $SbCl_6^-$ as red single crystals as the first example of a stable radical cation salt of an alkyl-substituted benzene. The X-ray crystallography which was conducted on this salt indicated that the bond lengths of the π-conjugated system become generally longer in the radical cation, as shown in Fig. 1.[13] Although the benzene ring was distorted from the original D_{3h} symmetry, this distortion was attributed to the crystal environmental effects, such as crystal packing forces, rather than to the static Jahn–Teller distortion.

By the action of FSO_3H under vacuum, benzene **9** was found to give the arenium ion **13**, which undergoes a rapid intermolecular protonation-deprotonation process (Scheme 3) with the activation energy E_a = 12.0 kcal mol^{-1}.[9b] This process was observable by ^{13}C NMR (68 MHz) at a temperature ranging from –20 to 45 °C. At the lower temperatures, the intramolecular hydrogen migration only at one side of the benzene ring became more prominent (Scheme 4).

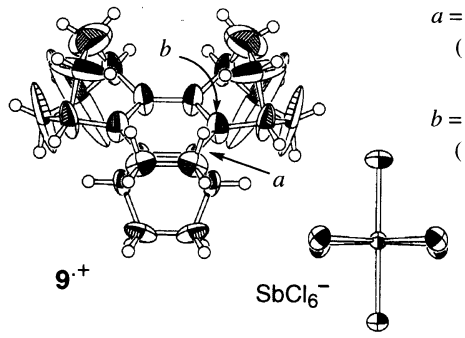

Fig. 1. ORTEP drawing of the X-ray structure of $\mathbf{9}^{\bullet+}SbCl_6^-$ with the averaged bond lengths. The values in the parentheses are the averaged bond lengths of the neutral molecule.

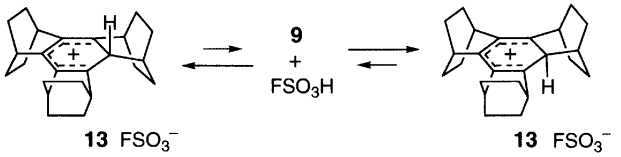

Scheme 3.

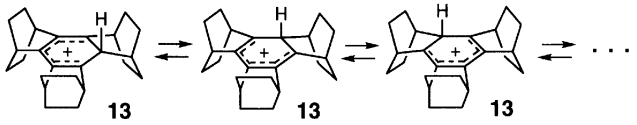

Scheme 4.

3. Polycyclic Aromatic Hydrocarbons Annelated with BCO

As to the polycyclic aromatic hydrocarbons annelated with BCO units, naphthalene **14**,[14] biphenylene **15**,[15] and anthracene **16**[16] were prepared. Naphthalene **14** was synthesized using a reaction of the BCO-annelated benzyne with the lithiated BCO dimer as the key step, as shown in Scheme 5.

Biphenylene **15** was formed by dimerization of the BCO-annelated benzyne (Scheme 6). On the other hand, anthracene **16** was synthesized by the Diels–Alder reaction between *para*-benzoquinone and BCO dimer as a key reaction, as shown in Scheme 7. The reactivity of **16** as a diene was found to be enhanced owing to the elevated HOMO level caused by the σ–π conjugation with the bicyclic σ-bonds. Thus, **16** can readily undergo a [4 + 2] cycloaddition with dicyanoacetylene or with tetracyanoethylene at room temperature.[16]

The structures of the hydrocarbons **14**–**16** were determined by X-ray crystallography. The π-conjugated systems were shown to be essentially planar. The intrinsic characteristics of the π-bond lengths of each aromatic compound were not affected by annelation with BCO groups, indicating that the annelation with BCO groups does not impose any strain on the ring systems.

All these polycyclic hydrocarbons were characterized by two-step one-electron oxidations with remarkably low oxidation potentials, as demonstrated by cyclic voltammetry (Table 2). Upon chemical oxidation with $SbCl_5$, all these hydrocar-

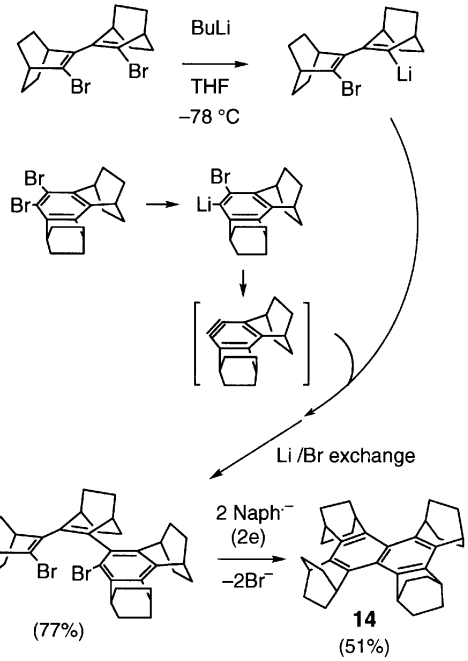

Scheme 5.

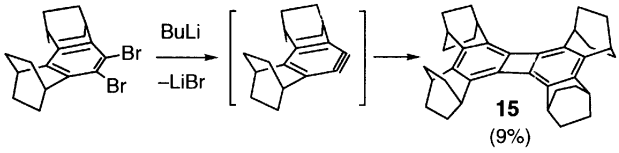

Scheme 6.

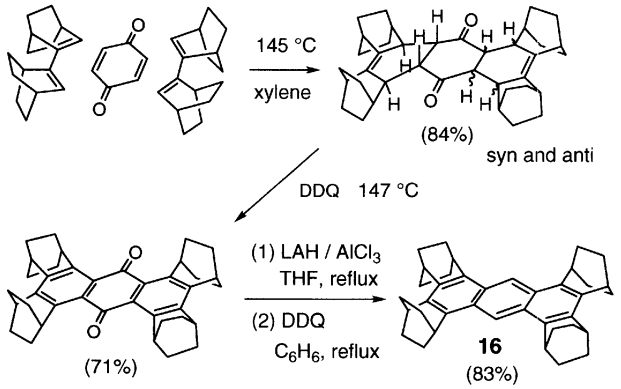

Scheme 7.

Table 2. Oxidation Potentials (V vs. Fc/Fc^+) of Naphthalene **14**, Biphenylene **15**, and Anthracene **16** Determined by Cyclic Voltammetry in 1,1,2,2-Tetrachloroethane[a)]

Compound	$E_{1/2}$ (1)[b)]	E_{pa} (2)[c)]
14	+0.33	+1.17
15	+0.25	+1.00
16	+0.17	+0.86

a) Ref. 13; Supporting electrolyte, Bu_4NClO_4 (0.1 mol dm^{-3}); scan rate, 20 mV s^{-1}. b) Half-wave potential; $(E_{pa}+E_{pc})/2$. c) Anodic peak potential.

bons gave isolable salts of the stable radical cations, which were dark green (**14**$^{\bullet+}$), blue violet (**15**$^{\bullet+}$), and dark green (**16**$^{\bullet+}$) in color. All these afforded air-stable single crystals and allowed the X-ray crystallography for the first time for the alkyl-substituted naphthalene and biphenylene radical cations.[13] The results are shown in Fig. 2. Here, the change in π-bond lengths upon one-electron oxidation of **14**–**16** is systematically related to the coefficients of the relevant carbons' HOMO of the neutral molecules (Fig. 3). The bonds with the bonding nature in the HOMO are elongated upon removal of one electron, i.e. one-electron oxidation, and those with antibonding in HOMO are shortened.

When treated with SbF_5, which has a stronger oxidizing power, these hydrocarbons are smoothly transformed into the corresponding dications, which can be characterized by ^{1}H NMR (Table 3) and ^{13}C NMR spectroscopies (Table 4). The dications of **14** and **16** exhibit the presence of a paramagnetic ring current because of the peripheral 8 and 12 π-electronic system, whereas the dication of **15** exhibits the presence of a diamagnetic ring current typical for a peripheral 10 π-system.

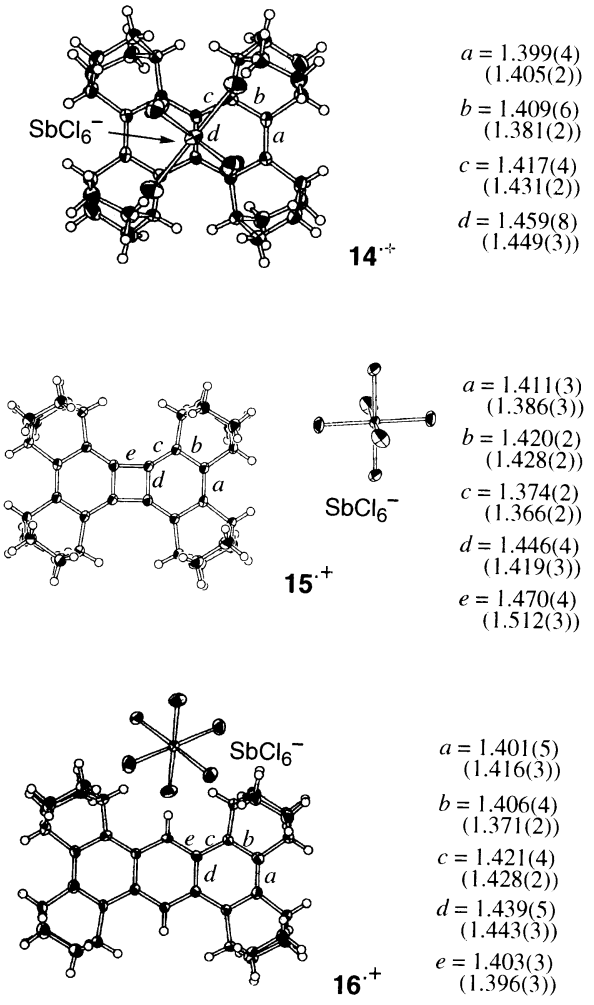

Fig. 2. ORTEP drawings of X-ray structures of **14**$^{\bullet+}$$SbCl_6^-$–**16**$^{\bullet+}$$SbCl_6^-$ with the averaged bond lengths. The values in the parentheses are the averaged bond lengths of the neutral molecules.

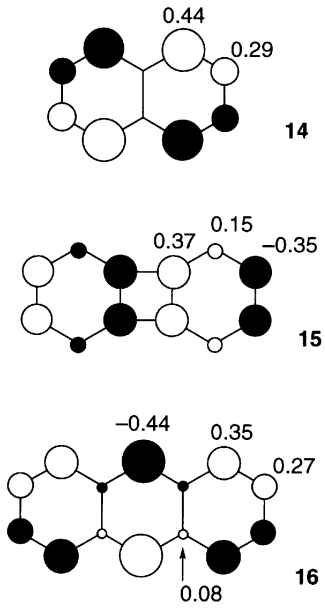

Fig. 3. HOMOs' coefficients of neutral **14**, **15**, and **16** calculated by B3LYP/6-31G*.

Table 3. ^{1}H NMR Data for Hydrocarbons **14**, **15**, and **16** in $CDCl_3$ and Their Dications **14**$^{2+}$, **15**$^{2+}$, and **16**$^{2+}$ in CD_2Cl_2

Compd	$\delta_{^1H}$/ppm			Ref.
	>CH	–CH	>CH$_2$	
14	—	3.78, 3.46	1.80, 1.40	14
14^{2+}	—	2.98, 2.88	2.13, 1.90	14
15	—	3.00, 2.81	1.73, 1.42	15
15^{2+}	—	4.19, 4.13	2.35, 1.71	–[a]
16	8.91	4.12, 3.53	1.89, 1.42	16
16^{2+}	8.74	3.58, 3.26	2.11, 1.76	16

a) A. Matsuura, T. Nishinaga, and K. Komatsu, unpublished.

4. Cycloheptatriene, Tropone, and Heptafulvene Annelated with BCO

The BCO-annelated benzene **9** can be ring-expanded to cycloheptatriene **17**, which undergoes rapid ring inversion (Scheme 8).[17] The energy barrier for ring inversion was determined as 8.5 kcal mol^{-1}, which is only 2.5 kcal mol^{-1} larger than that for the parent compound (6 kcal mol^{-1}).[18] This result suggests that the presence of the BCO groups does not substantially destabilize the planar transition-state structure by steric strain.

The cycloheptatriene **17** was oxidized by SeO_2 to the corresponding tropone **18**.[19] The basicity of tropone **18** was found to be nearly 2 p*K* unit larger than that of the parent compound,[20] indicating the effects of the BCO annelation to enhance the polarity of the molecule by stabilizing the positively polarized seven-membered ring. The heptafulvene derivative **19**[19] was

Table 4. ^{13}C NMR Data for Hydrocarbons **14**, **15**, and **16** in $CDCl_3$ and Their Dications $\mathbf{14}^{2+}$, $\mathbf{15}^{2+}$, and $\mathbf{16}^{2+}$ in CD_2Cl_2[a)]

Compd	$\delta_{^{13}C}$/ppm					Ref.
	C-1, C-2	C-4a	C-9	CH	CH_2	
14	135.32	125.1	—	32.7	26.6	14
	135.29			28.8	26.4	
$\mathbf{14}^{2+}$	210.8	154.0	—	41.9[b)]	25.9[b)]	14
	160.7			30.6[b)]	22.9[b)]	
15	136.6	140.4	—	31.3	26.4	15
	131.0			28.7	26.0	
$\mathbf{15}^{2+}$	159.9	183.8	—	38.1	26.8	—[b)]
	147.9			35.8	24.8	
16	135.5	115.5	136.1	29.3	27.0	16
	125.4			28.8	26.2	
$\mathbf{16}^{2+}$	160.9	131.0	181.9	32.9	24.1	16
	159.9			29.9	22.8	

a) Numbering system:

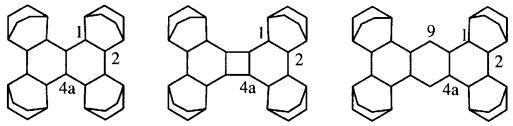

b) A. Matsuura, T. Nishinaga, and K. Komatsu, unpublished.

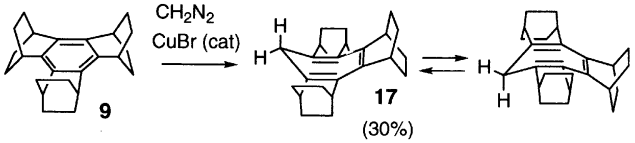

Scheme 8.

also found to be more polarized as compared with the parent compound,[21] as shown by ^{13}C NMR and IR spectra (Chart 2).

The low-temperature ^{13}C NMR indicated that the π-system of tropone **18** is planar, whereas that of heptafulvene **19** is in the boat conformation; the energy barrier for the ring inversion is 8.5 kcal mol^{-1}.[19]

5. Tropylium Ions Annelated with BCO

Cycloheptatriene **17** can be readily converted into tropylium ion **20**, which exhibits an extraordinarily high thermodynamic stability (Scheme 9).[22] The stabilization effect of each BCO unit is almost additive, and the pK_{R+} value of the tropylium ion **20** having three BCO groups amounts to 13.0 in 50% acetonitrile. This is the highest pK_{R+} value ever reported for substituted tropylium ions. Reflecting such stability, cation **20** does not react with typical nucleophiles such as N_3^- (pK_a of the conjugate acid, 4.59), $CH_3CO_2^-$ (4.76), CrO_4^{2-} (6.50), $C_6H_5S^-$ (6.50), SO_3^{2-} (7.21), $C_6H_5O^-$ (9.99), and CO_3^{2-} (10.33).[23] However, **20** does react with organolithium reagents at the 7-position and affords the tropylium ion derivatives **21**,[22] **22**,[24] **23**,[24] **24**,[24] and **25**[25] by the appropriate ionization method (Chart 3). The pK_{R+} and reduction potential data of these mono- and dications are given in Table 5.

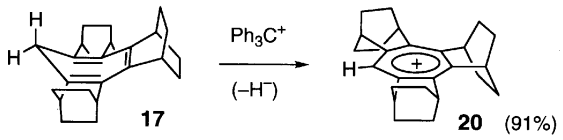

Scheme 9.

In spite of the presence of the electron-donating methyl substituent, cation **21** is less stable than **20**, probably due to the presence of too much steric congestion to maintain the planarity of the central tropylium ring. The benzene ring in cations **22**, **23**, and **24** is almost perpendicular to the plane of the tropylium ring, and destabilizes the cation due to the electron-withdrawing inductive effect.[24]

For the dication **25**, the X-ray crystallography study indicated that mean planes of the two tropylium rings are not coplanar

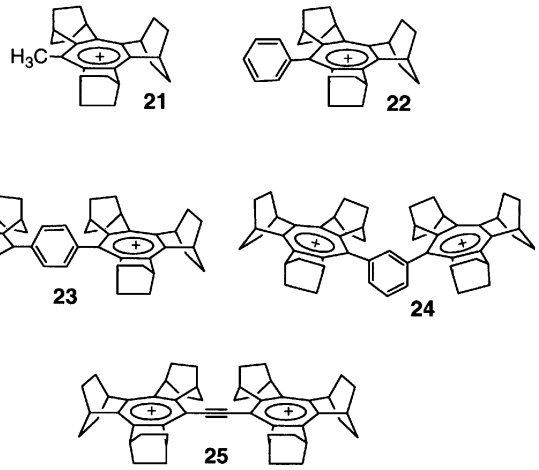

Chart 3.

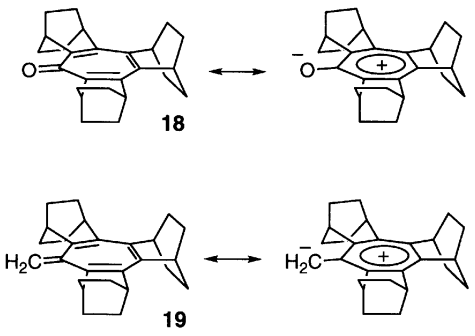

Chart 2.

Table 5. Values of pK_{R+} and Reduction Potential for the Tropylium Ions **20–25**

Cation	**20**	**21**	**22**	**23**	**24**	**25**
pK_{R^+}[a)]	13.0	12.4	12.0	11.5	10.4[b)]	7.0[b)]
					12.2	11.5
E_{red}[c)]	−1.12[d)]	−1.09[d)]	−1.12[e)]	−1.01[d)]	−1.14[e,f)]	−0.49[e,f)]
					−1.24	−0.66
Ref.	22	22	24	24	24	25

a) Measured in 50% aq MeCN. b) Two-step neutralization. c) V vs. Ag/Ag^+; measured in MeCN containing 0.1 mol dm^{-3} Bu_4NClO_4; scan rate, 0.1 V s^{-1}. d) Cathodic peak potential. e) Half-wave potential. f) Two-step reduction.

nor perpendicular, but are twisted with respect to each other with a dihedral angle of 44° (Fig. 4).[25] The repulsive interaction between the two tropylium rings in **25** results in considerable destabilization, as shown by the pK_{R^+} data.

Upon cyclic voltammetry, each of the two tropylium rings of dication **23** behaves independently and undergo one-electron reduction simultaneously. In contrast, each tropylium ring in **24** and **25** recognizes the other in the redox events and accepts two electrons in a stepwise manner.[24,25] Exhaustive electrolytic reduction of **24** produces a triplet diradical, as observed by ESR at –120 °C.[24] In contrast, the electrolytic reduction of **23** gives a closed-shell molecule which undergoes polymerization on the electrode.[24] The reduction of dication **25** affords a stable radical cation.[25]

6. Cyclooctatetraene Annelated with BCO

The dibromide of the BCO tetramer (**12**, $n = 4$) can be reductively cyclized to give cyclooctatetraene (COT) **26** (Scheme 10). As shown by the X-ray crystal structure (Fig. 5), **26** has a tub-shaped π-system typical for the COT ring.[26] Because of the steric constraint caused by the BCO annelation, a planar structure has a considerable angular strain and the ring inversion of the neutral COT **26** is inhibited, the energy barrier for ring inversion being estimated to be larger than 50 kcal mol^{-1} by both molecular orbital (PM3) and molecular mechanics calculations. Nevertheless, COT **26** (^{13}C NMR (THF-d_8) δ 140.0, 33.4, 26.6, and 25.8 ppm) can be reduced by potassium metal to give planar dianion **26**$^{2-}$, which exhibits only three ^{13}C NMR signals at δ 97.8, 35.8, and 30.6 ppm.[26] Apparently, the gain in the Hückel aromaticity (10 π-electron system) overcomes the angular strain in the planar system.

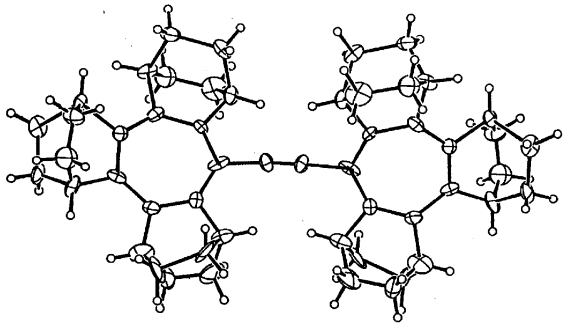

Fig. 4. ORTEP drawing of the X-ray structure of dication salt **25** $(SbF_6^-)_2$ (SbF_6^- is omitted for clarity).

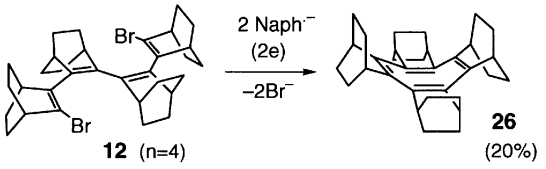

Scheme 10.

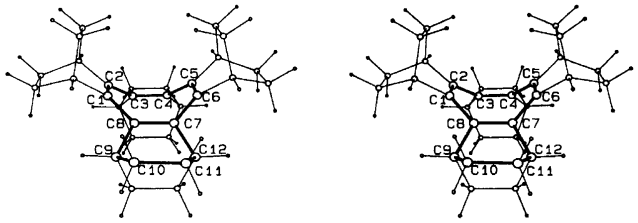

Fig. 5. Molecular structure of COT **26** (stereoview). Selected bond lengths (Å) and angles (°) are: C1–C2, 1.339(3); C2–C3, 1.465(2); C3–C4, 1.342(2); C4–C5, 1.469(2); C5–C6, 1.331(3); C6–C7, 1.464(2); C7–C8, 1.336(2); C8–C1, 1.475(2); C8–C9, 1.515(2); C9–C10, 1.544(4); C10–C11, 1.531(3); C6–C7–C8, 126.5(1); C7–C8–C1, 127.0(1); C7–C8–C9, 113.8(1); C8–C7–C12, 113.7(1).

Owing to the electronic effects of the BCO units, the levels of occupied molecular orbitals of COT **26** are raised, while those of unoccupied molecular orbitals are not affected. This is reflected in the cyclic voltammogram, which exhibited two consecutive reversible oxidation waves at such low potentials as +0.39 V and +1.14 V vs. Ag/Ag$^+$ in CH_2Cl_2–CF_3CO_2-H–$(CF_3CO)_2O$ (20:1:1).[27] In comparison, the parent COT only exhibits an irreversible oxidation peak at +1.20 V in acetonitrile. These results imply that the cationic species can be readily generated from COT **26**.

Compared with the anionic COT, the cationic species of COT has received only sporadic attention. The radical cation of the parent COT was predicted to be tub-shaped rather than planar by MNDO calculations.[28] However, the radical cation was so unstable that it could only be observed by flow ESR as a short-lived species.[29] The same species was also observed by electronic spectrum only at low temperature (–196 °C) in a Freon matrix.[30]

In sharp contrast, the COT **26** completely surrounded by BCO units afforded the first isolable salt of the stable radical cation **26**$^{\bullet+}$ by one-electron oxidation of **26** with $NO^+SbCl_6^-$ (Scheme 11).[31] X-ray crystallography data demonstrated that this radical cation has a tub-shaped eight-membered ring (Fig. 6), as has been predicted theoretically.[28]

The COT dication is a member of the Hückel aromatic system with six π electrons. There have been reported tetra- and di-substituted COT dications **27**$^{2+}$ and **28**$^{2+}$ which are stable only at low temperature (–78 °C) in the SO_2ClF solution.[32] At the temperatures above –20 °C, the dication rearranges into the bicyclic structure **29**$^{2+}$ (Chart 4).[32] On the other hand, when the radical cation of the BCO-annelated COT **26** was further oxi-

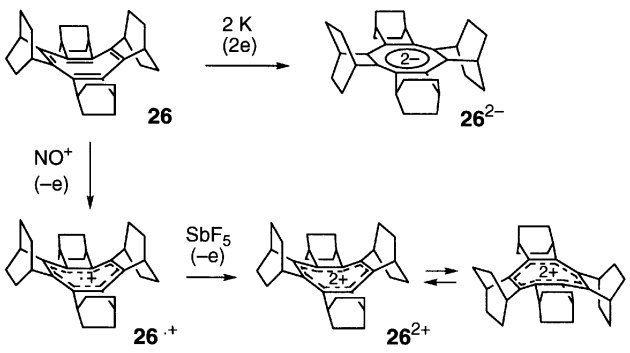

Scheme 11.

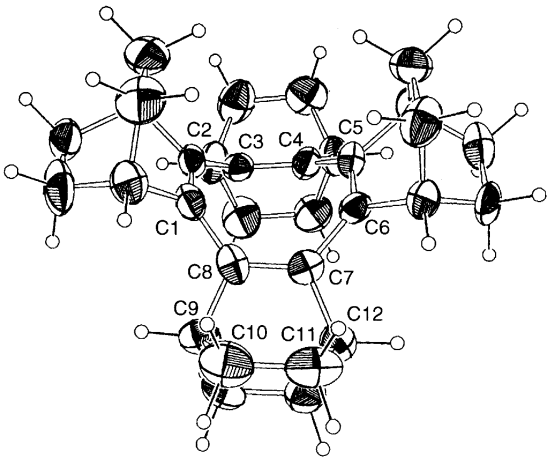

Fig. 6. ORTEP drawing of the X-ray structure of radical cation salt $\mathbf{26}^{\bullet+}SbCl_6^-$ ($SbCl_6^-$ is omitted for clarity). Selected bond lengths (Å) and angles (°) are: C1–C2, 1.389(10); C2–C3, 1.440(10); C3–C4, 1.356(10); C4–C5, 1.444(11); C5–C6, 1.377(10); C6–C7, 1.445(11); C7–C8, 1.338(11); C8–C1, 1.464(10); C8–C9, 1.529(10); C9–C10, 1.540(10); C10–C11, 1.537(13); C6–C7–C8, 126.1(7); C7–C8–C1, 127.9(7); C7–C8–C9, 114.1(6); C8–C7–C12, 113.8(8).

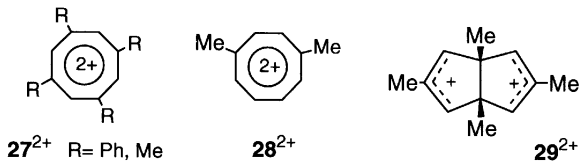

$\mathbf{27}^{2+}$ R= Ph, Me $\mathbf{28}^{2+}$ $\mathbf{29}^{2+}$

Chart 4.

dized with SbF_5 (Scheme 11), a stable dication was produced that exhibited only three ^{13}C NMR signals at δ 177.9, 41.0, and 23.9 ppm at room temperature. However, the signal for the methylene carbon atoms of the ethano bridge was split to give two signals at a low temperature (–80 °C), indicating that the ground-state structure of this dication is in the tub-structure, which is undergoing rapid ring inversion with an energy barrier of 10.8 kcal mol^{-1}.[27]

7. Pentamer of BCO Units

When the reductive cyclization was attempted on the dibromide of the BCO pentamer (**12**, $n = 5$) with sodium naphthalenide in THF at low temperature (–78 °C), a hydrocarbon product was obtained in 61% yield. The X-ray crystallography analysis indicated that this product was not the 10-membered ring compound but a bicyclo[2.2.2]octane having two spiro-connected cyclopentadiene rings at the vicinal carbons (**30**), as shown in Fig. 7.[33] The formation of **30** most probably proceeded, as shown in Scheme 12, by way of tandem double cyclization initiated by the σ-radical formed at one end of the BCO pentamer. The newly formed radical center can then attack the other end of the double bond to furnish two spiro-connected cyclopentadiene rings after further reduction. The second cyclization can alternatively be considered as a disrotatory electrocyclization

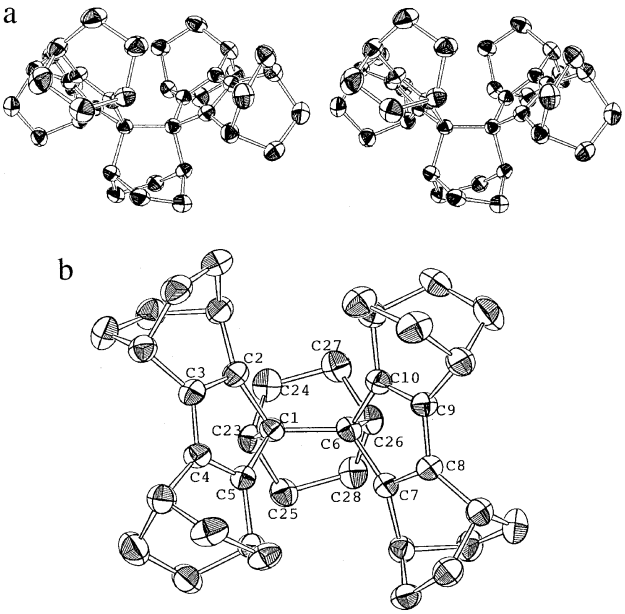

Fig. 7. ORTEP drawings of the X-ray structure of **30**: (a) a stereoview of the side view; (b) the top view. Hydrogens are omitted for clarity. Selected bond lengths (Å) and angles (°) are: C1–C2, 1.567(5); C2–C3, 1.356(4); C3–C4, 1.447(5); C4–C5, 1.341(5); C5–C1, 1.536(4); C1–C6, 1.627(4); C1–C23, 1.581(3); C23–C24, 1.531(5); C24–C27, 1.549(4); C27–C26, 1.526(5); C26–C6, 1.579(3); C1–C2–C3, 109.3(3); C2–C3–C4, 109.9(3); C3–C4–C5, 110.1(3); C4–C5–C1, 110.9(3); C5–C1–C6, 113.6(2); C2–C1–C6, 120.6(2); C6–C1–C23, 106.6(2); C1–C23–C24, 112.5(2); C1–C23–C25, 110.1(2).

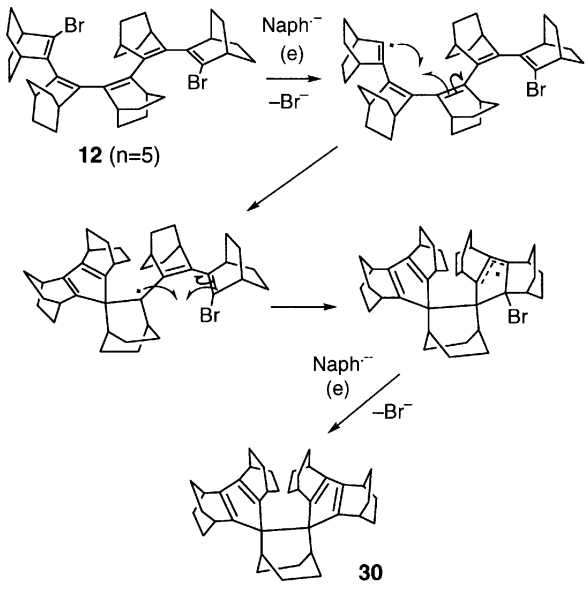

Scheme 12.

of the pentadienyl radical.

As shown in Fig. 7, hydrocarbon **30** has a highly congested structure with the two BCO-annelated cyclopentadiene rings

fixed in close proximity. In order to reduce the steric congestion, the two cyclopentadiene rings are skewed with each other and splayed out with the dihedral angle, between the mean planes of cyclopentadiene rings, of 86°.

The most remarkable feature in the structure of **30** is a significant elongation (1.627(4) Å) of the central single bond (C1–C6) connecting the two cyclopentadiene rings. This bond is much longer than the generally known value of 1.54 Å for single bonds between sp^3-hybridized carbons. At first sight, the most important factor for this bond elongation seems to be the steric one, that is, the release of severe steric congestion. In order to clarify the cause of this elongation, molecular mechanics calculations (MM2) were performed. The calculated structure fairly well reproduced the experimentally observed one except that the central σ-bond was calculated to be only 1.570 Å, which is 0.057 Å shorter than the observed value. This difference is attributed to an electronic effect, which was not fully taken into consideration in the MM2 calculations. Actually, the results of semiempirical molecular orbital calculations using MNDO for **30** gave a value of 1.632 Å for this central σ-bond, which is quite close to the observed one. From the consideration based on the calculations on relevant model compounds, it is assumed that the central σ-bond, which is in a geometry nearly parallel to the 2*p* orbitals of the two cyclopentadiene rings, is elongated due to C–C hyperconjugation with the 2*p* orbitals of the cyclopentadiene rings.

The central elongated single bond in **30** can be readily cleaved upon reduction with potassium metal in THF-d_8 in a vacuum-sealed tube to afford a solution of *cis*-1,4-cyclohexylenebis(cyclopentadienide) dianion **31**, as demonstrated by ^{13}C NMR spectrum (Scheme 13).[33]

8. Dehydroannulenes Annelated with BCO

A wide variety of dehydroannulenes have been synthesized and studied owing to the interest in their electronic structures[34] as well as in their supramolecular structures.[35] Dehydroannulenes fused with detachable cyclic units have been utilized as possible precursors of a new family of carbon allotropes, the cyclo[*n*]carbons.[36] In contrast to these studies, the annelation with BCO groups was expected to rigidly hold the π-system and to raise the HOMO level.

By the oxidative coupling under Eglinton conditions, the enediyne **32** was transformed into a series of dehydroannulenes annelated with BCO, **33**–**36** (Scheme 14).[37] On the other hand, the bromo(ethynyl) olefin **38** which was generated from **37** was coupled with itself by the use of CuI and Pd(0) catalysts to give dehydroannulenes **39** and **40** (Scheme 15).[37] From the molecular modeling and X-ray crystallography of some of the compounds, the cyclic π-systems in **33**, **34**, and **39** are considered

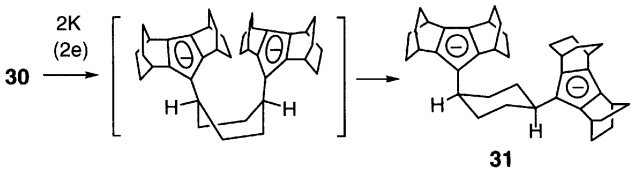

Scheme 13.

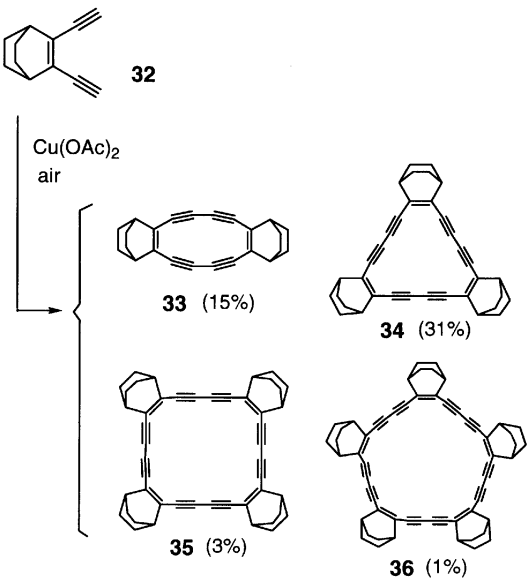

Scheme 14.

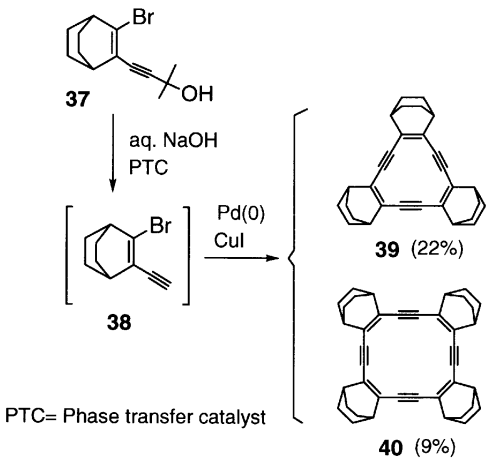

Scheme 15.

to be essentially planar, while those in **35**, **36**, and **40** have folded structures. The redox potentials of these and one parent dehydroannulenes (**41**) are shown in Table 6. Upon comparison of the antiaromatic planar dehydroannulenes having 12 π-electrons, the one having three BCO units (compound **39**) apparently has the lowest oxidation potential, i.e., the highest tendency to be oxidized. This can be taken as the characteristic of the BCO annelation effect.

The raising of the HOMO level particularly in annulene **40** was also demonstrated by complexation of a silver ion (AgOTf or $AgSbF_6$) in its cavity, as shown in Fig. 8.[38] The silver ion is present in the center of the cavity and the counter anions are located above the silver ion. The structure of the central ring of the annulene is still tub-like, but the folding angles are smaller compared with the structure of **40** itself. The complexation with $AgSbF_6$ was found to be stronger, the Ag–C(alkyne) distances being shorter particularly for one set of the opposing acetylene linkages. The results of theoretical calculations indicated that this annulene-type ligand reduces the positive charge

Table 6. Redox Potentials ($E_{1/2}$, V vs. Ag/Ag$^+$) of Dehydroannulenes Determined by Cyclic Voltammetry in Benzonitrile[a)]

Compd	E_{red}	E_{ox}
41[e)]	−1.58	+1.17[b)]
33	−1.67	+0.93[b)]
34	−1.96	+1.21[b)]
35[c)]	−1.53	—
36	−1.90[b)]	+1.07[b)]
39	−1.93	+0.54
40	−1.96	+0.62[d)]

a) Ref. 37. Supporting electrolyte, Bu_4NClO_4 (0.1 mol dm^{-3}); scan rate 0.1 V s^{-1}. b) Peak potential of the irreversible peak. c) Because of the low solubility, the measurement was performed in benzonitrile–dichloromethane (4 : 3). The observable range in this solvent was from +1.0 V to −2.0 V. d) The second irreversible peak was observed at +0.88 V. e)

41

on the silver atom; the extent of this reduction is larger for the case of $AgSbF_6$.

9. 1,4-Dithiin Annelated with BCO

The study has been extended to the sulfur-containing π-conjugated system. 1,4-Dithiin is considered as an 8 π-electron antiaromatic system with high π-donor ability. Compared with its dibenzo-homologue, thianthrene, the alkyl substituted 1,4-dithiin has received much less attention.[39] The 1,4-dithiin annelated with two BCO units **42** was synthesized as yellow crystals by the reaction of bis(3-oxobicyclo[2.2.2]oct-2-yl) sulfide with Lawesson's reagent, as shown in Scheme 16.[40]

The cyclic voltammetry of dithiin **42** exhibited a reversible first oxidation wave at a remarkably low potential of $E_{1/2}$ +0.00 V vs. Fc/Fc$^+$ and an irreversible second oxidation peak at E_{pa} +0.84 V. The second oxidation peak became reversible when the measurement was conducted at low temperature (–78 °C) under vacuum. Reflecting the low oxidation potentials, dithiin **42** readily underwent one-electron oxidation with 3 molar equivalents of SbF_5 to give the radical cation salt **42**$^{\bullet+}$ SbF_6^- as brown crystals in 67% yield. This salt was so stable that no decomposition was observed upon standing in air for several days.

As shown by the molecular structure of **42**$^{\bullet+}$ SbF_6^- (Fig. 9) determined by X-ray crystallography, the dithiin ring was found to be planar and the C–S bond was markedly shortened in the radical cation. The ESR spectrum of the radical cation **42**$^{\bullet+}$ exhibited a nine-line signal due to the coupling with eight *anti*-protons of the ethano bridges. A coupling with ^{33}S was also observed with a coupling constant (0.86 mT) which is smaller than that observed in the case of thianthrene radical cation (0.92 mT).[41] This result indicates that the ability of the BCO units to delocalize the positive charge and an unpaired electron is even more significant than that of the annelated benzene rings.

The two-electron oxidation of dithiin **42** with excess of SbF_5 in CD_2Cl_2 at ambient temperature gave an orange solution,

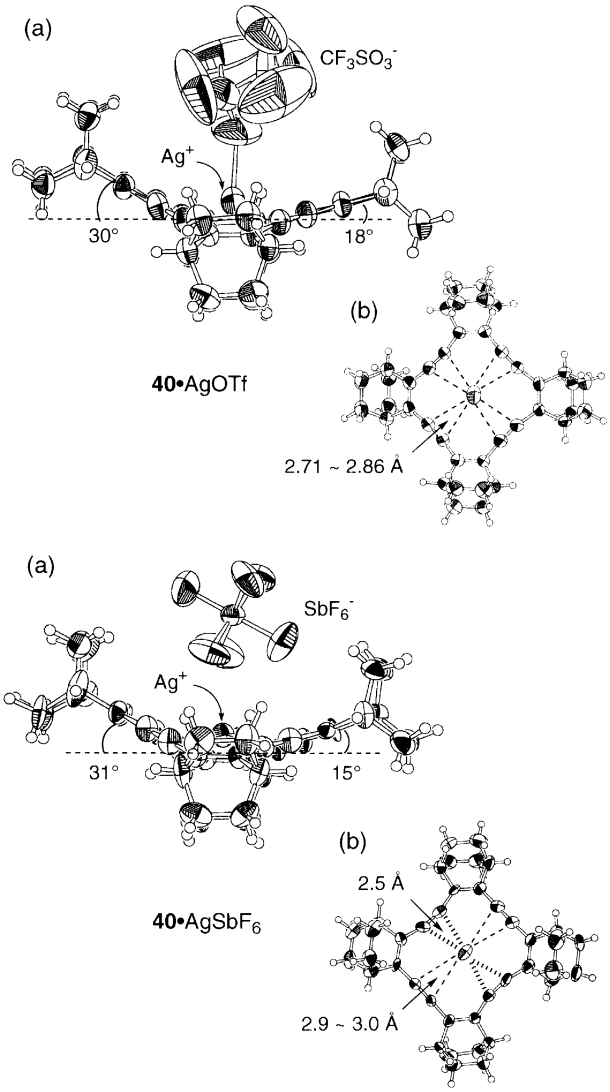

Fig. 8. ORTEP drawings of the X-ray structures of **40**·AgOTf and **40**·$AgSbF_6$. (a) Side views and (b) top views.

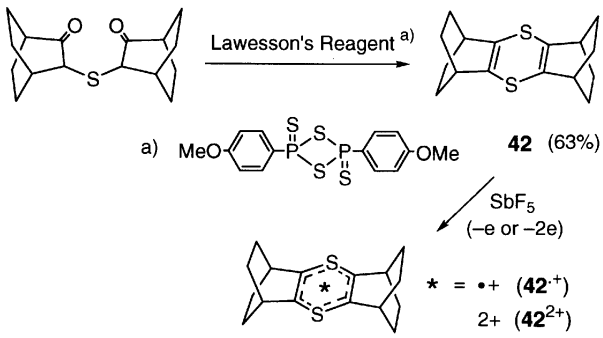

Scheme 16.

which exhibited ^1H and ^{13}C NMR signals at a considerably lower field than that with neutral **42**, as shown in Table 7.[42] The observed chemical shifts were in fair agreement with the calcu-

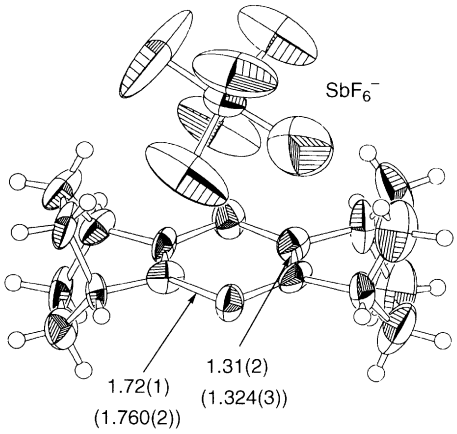

Fig. 9. ORTEP drawing of the X-ray structure of radical cation salt $\mathbf{42}^{\bullet+}SbF_6^-$. The values in prentheses are bond lengths of neutral **42** in Å.

Table 7. ^{1}H and ^{13}C NMR Chemical Shifts (ppm) for 1,4-Dithiin **42** and Its Dication $\mathbf{42}^{2+}$

Compd		^{1}H NMR		^{13}C NMR		
		CH	CH_2	C=C	CH	CH_2
42	obsd[a]	2.46	1.53 (8H) 1.33 (8H)	128.4	38.1	26.2
$\mathbf{42}^{2+}$	obsd[a]	4.48	2.47 (8H) 1.86 (8H)	180.0	43.0	25.1
	calcd[b]	4.18	2.84 (*anti*) 1.66 (*syn*)	197.0	38.7	22.2

a) In CD_2Cl_2. b) GIAO/ HF/ 6-31+G*// B3LYP/ 6-31G*.

lated values for the dication $\mathbf{42}^{2+}$. The signal of bridgehead protons which are located in the plane of the dithiin's π-system exhibited a marked downfield shift of 2 ppm as compared with that of neutral **42**. This clearly indicates the presence of a diamagnetic ring current in the dicationic dithiin ring and the aromatic character in this 6 π-electronic system.

10. Silacycloheptatrienes and Silatropylium Ion Annelated with BCO

The study was further extended to the seven-membered ring system containing Group 14 elements. The dibromide of BCO trimer **12** ($n = 3$) was lithiated at the both ends and was allowed to react with dichlorides of Group 14 elements, as shown in Scheme 17, to give a series of metallacycloheptatrienes (metallepins) containing silicon (**43b**), germanium (**44**), and tin (**45**).[43]

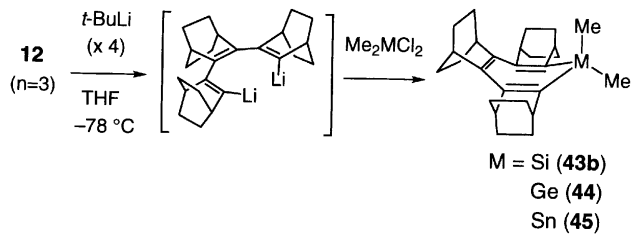

Scheme 17.

The molecular structures of these metallepins were determined by X-ray crystallography as the boat form, which differed only in the length of the metal–C1 bond and the folding angle of the boat. The structure of **43b** is shown in Fig. 10 for one example. The metal–C1 bond length was elongated in the order, M = Si (1.857(2) Å), Ge (1.926(3) Å), Sn (2.108(9) Å), and the folding angle near the bow of the boat form decreased in this order. The ^{1}H NMR results indicated that these metallepins undergo rapid ring inversion (Scheme 18). The energy barrier for this process was determined by a variable-temperature NMR technique to give the activation parameters shown in Table 8. Apparently, the energy barrier increased as the atomic size of the Group14 element increased. This is primarily attributed to the increase in strain in the planar structure at the transition state: the larger strain is generated by elongation of the M–C1 bond that demands widening of inner angles in the planar seven-membered ring.

In the same manner as Scheme 17 shown above, a series of silacycloheptatrienes (silepins) having various electron-donating and -withdrawing substituents on silicon, **43a**–**43g**, were synthesized from the BCO trimer **12** ($n = 3$).[44] The energy bar-

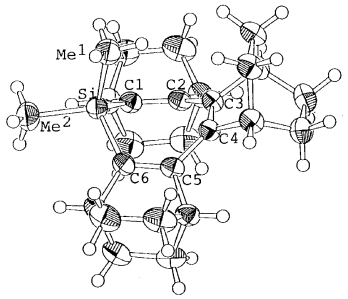

Fig. 10. ORTEP drawing of the X-ray structure of **43b**. Selected bond lengths (Å) and angles (°) are: Si–Me^1, 1.875(4); Si–Me^2, 1.869(4); Si–C1, 1.857(2); C1–C2, 1.350(3); C2–C3, 1.461(3); C3–C4, 1.363(4); C1–Si–C6, 103.2(1); Si–C1–C2, 120.6(2); C1–C2–C3, 126.6(2); C2–C3–C4, 128.3(1).

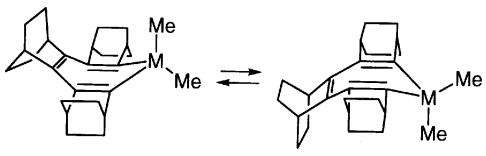

Scheme 18.

Table 8. Activation Parameters (25 °C) for the Ring Inversion of Cycloheptatriene **17** and Metallepins **43b**, **44**, and **45**

Compd	$\Delta H^{\ddagger}$[a]	$\Delta S^{\ddagger}$[b]	$\Delta G^{\ddagger}$[a]
17[c]	7.9 ± 0.5	−11 ± 3	11.3 ± 0.2
43b[d]	13.4 ± 1.3	3 ± 5	12.4 ± 0.2
44[d]	16.0 ± 1.8	7 ± 6	14.0 ± 0.1
45[d]	21.3 ± 3.0	10 ± 9	18.4 ± 0.5

a) In kcal mol^{-1}. b) In cal K^{-1} mol^{-1}. c) Ref. 17. d) Ref. 43.

rier for the ring inversion of these silepins was measured by a variable-temperature NMR technique. The results are shown in Table 9 together with the positive charge on silicon atom calculated by semi-empirical molecular orbital method (PM3). There is a qualitative correlation that the $\Delta G^{\ddagger}$ value for ring inversion of silepins decreases as the substituent on silicon becomes more electronegative and generates greater positive charge on the silicon atom. This decrease in energy barrier for ring inversion can be ascribed to the relative stabilization of the tropylium-ion-like electronic structure at the planar transition state caused by the electronegative substituents on silicon.[44] In these studies, the annelation with BCO units turned out to be suitable for placing the energy barrier of ring inversion within an experimentally measurable range. Without the BCO units, the ring inversion of unsubstituted silepin was calculated to be as low as 0.9 kcal mol^{-1}.[45]

In the above study, the "tropylium-ion-like" electronic structure was supposed to be present in the planar transition state. Now a question arises whether it is possible to generate the tropylium ion containing silicon in its conjugated system, i.e. the "silatropylium ion". The preparation of non-coordinated silylium ion has been one of the most challenging subjects in organosilicon chemistry. So far the studies on observation or preparation of such silylium ions have been limited to only three reports.[46,47,48] Even in the gas phase, a suggestion of the silatropylium ion as one of the $C_6H_7Si^+$ isomers observed in a FT ICR mass spectrum[49] was disproved by a subsequent experimental study showing that it was a rearranged isomer $C_6H_6{\cdot}SiH^+$.[50] We have attempted to generate the silatropylium ion by virtue of stabilization by annelation with BCO units and steric protection with a bulky substituent on silicon.

Thus, dichlorosilepin **43f** was transformed into silepin **46** having a mesityl group on silicon, as shown in Scheme 19. The hydride abstraction from **46** using triphenylmethyl tetrakis(pentafluorophenyl)borate (Ph_3C^+ $TPFPB^-$) in CD_2Cl_2 at low temperature (–60 °C) successfully afforded a solution of

Table 9. Energy Barrier for Ring Inversion ($\Delta G^{\ddagger}$/kcal mol^{-1}) Determined by VT NMR and Positive Charge on Silicon Calculated by PM3[a)]

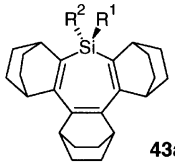

43a-g

	Compd R^1	R^2	$T_{coales.}$[b)]/°C	$\Delta G^{\ddagger}$[c)]	δ + (Si)
43a	H	*t*-Bu	>20	>14.1	+0.47
43b	Me	Me	−17	12.4	+0.50
43c	H	Me	−20	11.9	+0.51
43d	H	H	−40	11.1	+0.52
43e	MeO	MeO	−55	10.3	+0.90
43f	Cl	Cl	−80	9.6	+0.88
43g	F	F	−105	8.2	+0.96

a) Ref. 44. b) Coalescence temperature. c) Value at the coalescence temperature.

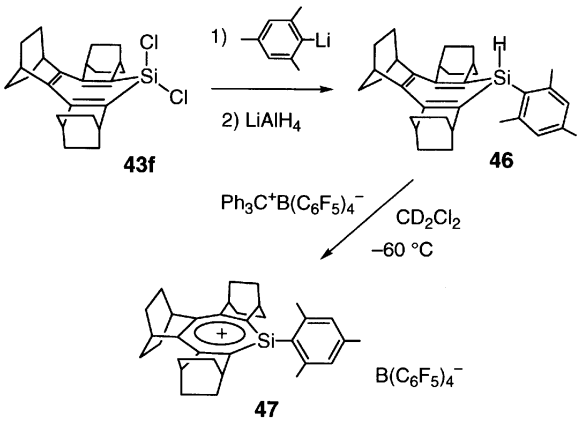

Scheme 19.

Table 10. ^{13}C NMR Chemical Shifts (δ/ppm) for Silatropylium ion **47** at −50 °C in CD_2Cl_2[a)]

C(sp^2)		C(sp^3)		
Tropyl	Aryl	CH	CH_2	CH_3
175.9	144.8	36.8	25.1	25.9
153.2	143.8	35.1	24.2	21.4
149.7	128.0	34.9	23.9	
	118.7			

a) Ref. 51.

the BCO-annelated silatropylium ion **47**, which was confirmed by the ^1H NMR (CD_2Cl_2) δ 7.13 (2H), 3.70 (2H), 3.64 (2H), 3.21 (2H), 2.41 (6H), 2.36 (3H), 1.9–1.7 (12H), 1.4–1.2 (12H)) and ^{13}C NMR data (Table 10).[51] The ^{29}Si NMR signal was observed at δ 142.9, which is 192.2 ppm down-field shifted compared with the precursor silepin **46** (δ −49.3). The signals for the BCO's bridgehead protons of **47** are also about 1 ppm down-field shifted compared with those for **46**. This is taken as the experimental proof for the presence of aromatic ring current in **47**. Although the cation **47** is stable only at the low temperature and slowly abstracts chloride ion from the solvent CD_2Cl_2, this study clearly demonstrated that such an unusual species as the silatropylium ion can be realized by virtue of annelation with BCO units which rigidly hold the π-conjugated system and of the presence of a bulky substituent such as the mesityl group on silicon.

The author sincerely thanks all the co-workers and students whose names appear in the references and who devoted themselves to the present study. The financial support by Grants-in-Aid for Scientific Research from the Ministry of Education, Science, Sports and Culture is gratefully acknowledged.

References

1 P. v. R. Schleyer, J. W. de M. Carneiro, W. Koch, and D. A. Forsyth, *J. Am. Chem. Soc.*, **113**, 3990 (1991).
2 T. Laube, *Angew. Chem., Int. Ed. Engl.*, **25**, 349 (1986).
3 S. Nelsen, M. F. Teasley, D. L. Kapp, C. R. Kessel, and L. A.

Grezzo, *J. Am. Chem. Soc.*, **106**, 791 (1984).

4 K. Komatsu, K. Takeuchi, M. Arima, Y. Waki, S. Shirai, and K. Okamoto, *Bull. Chem. Soc. Jpn.*, **55**, 3257 (1982).

5 K. Komatsu, H. Akamatsu, and K. Okamoto, *Tetrahedron Lett.*, **28**, 5889 (1987).

6 a) N. L. Frank, K. K. Baldridge, and J. S. Siegel, *J. Am. Chem. Soc.*, **117**, 2102 (1995). b) H-B. Bürgi, K. K. Baldridge, K. Hardcastle, N. L. Frank, P. Gantzel, J. S. Siegel, and J. Ziller, *Angew. Chem., Int. Ed. Engl.*, **34**, 1454 (1995).

7 P. G. Gassman and I. Gennick, *J. Am. Chem. Soc.*, **102**, 6863 (1980).

8 R. Durr, O. D. Lucchi, S. Cossu, and V. Lucchini, *Chem. Commun.*, **1996**, 2447.

9 a) K. Komatsu, Y. Jinbu, G. R. Gillette, and R. West, *Chem. Lett.*, **1988**, 2029. b) K. Komatsu, S. Aonuma, Y. Jinbu, R. Tsuji, C. Hirosawa, and K. Takeuchi, *J. Org. Chem.*, **56**, 195 (1991).

10 K. Shahlai and H. Hart, *J. Am. Chem. Soc.*, **110**, 7136 (1988).

11 S. Cossu, O. D. Lucchi, V. Lucchini, G. Valle, M. Balci, A. Dastan, and B. Demirci, *Tetrahedron Lett.*, **38**, 5319 (1997).

12 R. Rathore, S. V. Lindeman, A. S. Kumar, and J. K. Kochi, *J. Am. Chem. Soc.*, **120**, 6012 (1998).

13 A. Matsuura, T. Nishinaga, and K. Komatsu, *J. Am. Chem. Soc.*, **122**, 10007 (2000).

14 A. Matsuura, T. Nishinaga, and K. Komatsu, *Tetrahedron Lett.*, **38**, 3427 (1997).

15 A. Matsuura, T. Nishinaga, and K. Komatsu, *Tetrahedron Lett.*, **38**, 4125 (1997).

16 A. Matsuura, T. Nishinaga, and K. Komatsu, *Tetrahedron Lett.*, **40**, 123 (1999).

17 S. Aonuma, K. Komatsu, and K. Takeuchi, *Chem. Lett.*, **1989**, 2107.

18 a) F. A. L. Anet, *J. Am. Chem. Soc.*, **86**, 458 (1964). b) F. R. Jensen and L. A. Smith, *J. Am. Chem. Soc.*, **86**, 956 (1964).

19 S. Aonuma, K. Komatsu, N. Maekawa, and K. Takeuchi, *Chem. Lett.*, **1991**, 767.

20 a) D. J. Bertelli and T. G. Andrews, Jr., *J. Am. Chem. Soc.*, **91**, 5280 (1969). b) D. J. Bertelli, T. G. Andrews, Jr., and P. O. Crews, *J. Am. Chem. Soc.*, **91**, 5286 (1969). c) R. L. Redington, S. A. Latimer, and C. W. Bock, *J. Phys. Chem.*, **94**, 163 (1990).

21 a) W. von E. Doering and D. H. Wiley, *Tetrahedron*, **11**, 183 (1960). b) R. Hollenstein, A. Mooser, M. Neuenschwander, and W. von Philipsborn, *Angew. Chem.*, **86**, 595 (1974). c) W. K. Schenk, R. Kyburz, and M. Neuenschwander, *Helv. Chim. Acta*, **58**, 1099 (1975).

22 K. Komatsu, H. Akamatsu, Y. Jinbu, and K. Okamoto, *J. Am. Chem. Soc.*, **110**, 633 (1988).

23 K. Komatsu, H. Akamatsu, S. Aonuma, Y. Jinbu, N. Maekawa, and K. Takeuchi, *Tetrahedron*, **47**, 6951 (1991).

24 K. Komatsu, T. Nishinaga, N. Maekawa, A. Kagayama, and K. Takeuchi, *J. Org. Chem.*, **59**, 7316 (1994).

25 A. Kagayama, K. Komatsu, T. Nishinaga, K. Takeuchi, and C. Kabuto, *J. Org. Chem.*, **59**, 4999 (1994).

26 K. Komatsu, T. Nishinaga, S. Aonuma, C. Hirosawa, K. Takeuchi, H. J. Lindner, and J. Richter, *Tetrahedron Lett.*, **32**, 6767 (1991).

27 T. Nishinaga, K. Komatsu, and N. Sugita, *Chem. Commun.*, **1994**, 2319.

28 M. J. S. Dewar, A. Harget, and E. Haselbach, *J. Am. Chem. Soc.*, **91**, 7521 (1969).

29 R. M. Dessau, *J. Am. Chem. Soc.*, **92**, 6356 (1970).

30 T. Shida and S. Iwata, *J. Am. Chem. Soc.*, **95**, 3473 (1973).

31 T. Nishinaga, K. Komatsu, N. Sugita, H. J. Lindner, and J. Richter, *J. Am. Chem. Soc.*, **115**, 11642 (1993).

32 a) G. A. Olah, J. S. Staral, and L. A. Paquette, *J. Am. Chem. Soc.*, **98**, 1267 (1976). b) G. A. Olah, J. S. Staral, G. Liang, L. A. Paquette, W. P. Melega, and M. J. Carmody, *J. Am. Chem. Soc.*, **99**, 3349 (1977).

33 K. Komatsu, T. Nishinaga, K. Takeuchi, H. J. Lindner, and J. Richter, *J. Org. Chem.*, **59**, 7322 (1994).

34 a) F. Sondheimer, *Pure Appl. Chem.*, **28**, 331 (1971). b) M. Nakagawa, *Pure Appl. Chem.*, **44**, 885 (1975).

35 a) T. C. Bedard and J. S. Moore, *J. Am. Chem. Soc.*, **117**, 10662 (1995). b) Z. Wu and J. S. Moore, *Angew. Chem., Int. Ed. Engl.*, **35**, 297 (1996). c) A. S. Shetty, J. Zhang, and J. S. Moore, *J. Am. Chem. Soc.*, **118**, 1019 (1996).

36 a) F. Diederich, Y. Rubin, C. B. Knobler, R. L. Whetton, K. E. Schriver, K. N. Houk, and Y. Li, *Science*, **245**, 1088 (1989). b) F. Diederich and Y. Rubin, *Angew. Chem., Int. Ed. Engl.*, **31**, 1101 (1992). c) Y. Tobe, H. Matsumoto, K. Naemura, Y. Achiba, and T. Wakabayashi, *Angew. Chem., Int. Ed. Engl.*, **35**, 1800 (1996).

37 T. Nishinaga, T. Kawamura, and K. Komatsu, *J. Org. Chem.*, **62**, 5354 (1997).

38 T. Nishinaga, T. Kawamura, and K. Komatsu, *Chem. Commun.*, **1998**, 2319.

39 G. Klar in "Methods of Organic Chemistry," ed by E. Schaumann, Thieme, Stuttgart, (1997), Vol. E9a, p. 250.

40 T. Nishinaga, A. Wakamiya, and K. Komatsu, *Tetrahedron Lett.*, **40**, 4375 (1999).

41 P. D. Sullivan, *J. Am. Chem. Soc.*, **90**, 3618 (1968).

42 T. Nishinaga, A. Wakamiya, and K. Komatsu, *Chem. Commun.*, **1999**, 777.

43 T. Nishinaga, K. Komatsu, and N. Sugita, *J. Org. Chem.*, **60**, 1309 (1995).

44 T. Nishinaga, Y. Izukawa, and K. Komatsu, *Chem. Lett.*, **1998**, 269.

45 T. Nishinaga, Y. Izukawa, and K. Komatsu, *J. Phys. Org. Chem.*, **11**, 475 (1998).

46 J. B. Lambert and Y. Zhao, *Angew. Chem., Int. Ed. Engl.*, **36**, 400 (1997).

47 H.-U. Steinberger, T. Müller, N. Auner, C. Maerker, and P. v. R. Schleyer, *Angew. Chem., Int. Ed. Engl.*, **36**, 626 (1997).

48 A. Sekiguchi, T. Matsuno, and M. Ichinohe, *J. Am. Chem. Soc.*, **122**, 11250 (2000).

49 a) S. Murthy, Y. Nagano, and J. L. Beauchamp, *J. Am. Chem. Soc.*, **114**, 3573 (1992). b) Y. Nagano, S. Murthy, and J. L. Beauchamp, *J. Am. Chem. Soc.*, **115**, 10805 (1993).

50 R. L. Jarek and S. K. Shin, *J. Am. Chem. Soc.*, **119**, 6376 (1997).

51 T. Nishinaga, Y. Izukawa, and K. Komatsu, *J. Am. Chem. Soc.*, **122**, 9312 (2000).

Koichi Komatsu was born in 1942 in Kyoto. After spending one year at Davidson College, NC, USA, he graduated from Kyoto University in 1966. He studied at the graduate school of Kyoto University and became an instructor in 1971. He received his doctorate degree for his studies on one-electron reduction of carbocations in 1974. Then he carried out post-doctoral studies on polyquinocycloalkanes with Professor Robert West at the University of Wisconsin, Madison, USA, in 1975-1976. He returned to Kyoto University and, after serving as a lecturer (1984–1989) and an associate professor at the Department of Hydrocarbon Chemistry (1989–1993) and at the Institute for Chemical Research (1993–1995), he became a professor at the Institute for Chemical Research of Kyoto University in 1995. His research is concerned with carbocation chemistry, the structural studies and physical organic studies on cyclic π-conjugated systems, and the fullerene chemistry. He received the Divisional Award of the Chemical Society of Japan for the year 1997.